# EXPERIMENTAL STUDY OF MULTIPHASE PUMPING IN PROGRESSIVE CAVITY PUMPS

**G.M. Bessa, bessa@puc-rio.br**
**A.M. Athayde, arthur_hari@hotmail.com**
**L.F.A Azevedo, lfaa@puc-rio.br**
Department of Mechanical Engineering, PUC-Rio, Rio de Janeiro, RJ 22453-900, Brazil

***Abstract****. Progressive Cavity Pumps (PCP) have been extensively employed in different applications such as pumping abrasive or multiphase fluids, oil well fluids or even food products. In the last few years, the usage of the PCP in the oil & gas industry has increased due to its multiphase pumping capability. The pumping principle that makes PCP so useful is based on the displacement of discrete cavities formed between the rotor (single helical gear) and the stator (double helical gear). Hence, it is a fixed flow rate pump as the flow rate is directly associated with the rotation of the rotor. In this research we studied the performance of a PCP operating with single and two-phase flow of air and water. Our aim was to obtain the pressure and temperature profiles along the stages of the pump's stator, and to observe the influence on its hydrodynamic performance due to different variables such as gas void fraction (GVF), rotational speed and pressure gradient (ΔP). The information obtained from this study, is useful to assess how flow conditions affect the pump's life and performance and to validate numerical simulations conducted in the same research project, but not reported in the present paper. The PCP tested had seven stages, and a 38-mm-diameter rotor. Pressure and temperature measurements were performed in the interior of each of the pump cavities employing capacitive pressure transducers and fine-gauge thermocouples. The pump tests were conducted to obtain the volumetric flow, pressure and temperature, power, efficiency and slip versus ΔP along the stator for various shaft speeds. The results obtained demonstrated that as ΔP increases, the maximum pressure point displaces toward the pump outlet, reaching it at a higher ΔP. The useful power for two-phase flow decreases as the gas void fraction (GVF) increases in the flow. In the other hand, the useful power increases as shaft rotation speed increases. The volumetric efficiency of the pump is a strong function of the mixture compressibility. In fact, the greatest differences in volumetric efficiency between single-phase and two-phase flow are found in experiments where the gas void fraction is higher and for lower operating pressures. Under these conditions the mixture is very compressible which causes a decrease in volumetric efficiency. For higher levels of output pressure, the difference in volumetric efficiency is lower due to the higher density of the gas phase. For single-phase fluid the slip flow (flow that slips by the sealing line) decreases as shaft rotation speed increases. In the case of mixed phases, the compressibility of gas accommodates part of the return flow of the liquid phase, which does not necessarily mean a slip flow of liquid across the pump against to the main stream flow, as in the case of single-phase operation with liquid. The fluid temperature for single-phase flow increases as ΔP increases. Moreover, for two-phase flow, the fluid temperature increases as GVF increases. As the pressure at the pump discharge is progressively increased, the GVF in cavities subjected to higher levels of pressure decreases strongly due to the effect of gas compressibility.*

***Keywords:*** *Progressive Cavity Pumps, Petroleum artificial lift, Multiphase flow pumping*

## 1. INTRODUCTION

Multiphase pumping employing Progressive Cavity Pumps (PCP) has emerged as alternative for production and transportation of crude oil. The use of multiphase pumping technology offers the advantage of lowering the production costs as a consequence of the reduced amount of required equipment. Indeed, with this technology pump, compressor, separator, gas pipeline and liquid pipeline used in conventional setups can be replaced by a single pipeline and one PCP.

The PCP consists of a single helical gear (rotor) which rotates eccentrically inside a double helical elastomeric gear (stator) of the same minor diameter and twice the pitch length, and it can be used to pump a wide range of multiphase mixtures, including high viscosity fluids with entrained gas and solid particles in suspension. However, PCP's have a reduced ability to handle flows presenting high gas-liquid ratios due to limitations in the thermo-mechanical properties of the elastomers used for manufacturing the stator. The present paper presents a contribution to the study of PCP's performance operating at high gas-liquid ratios. Pump performance was determined for flows ranging from water in single phase, to two-phase flow of air and water with gas volume fractions (GVF) up to 50%. Specifically, the focus of this experimental investigation was on the effect of gas volume fraction on the temperature and pressure axial distribution along the pump's cavities. The influence of gas volume fraction on global pump performance was also studied

The literature on the analysis of PCP's performance operating in two-phase flow is scarce. The work of Martin et al., 1999 presents extensive experimental studies dedicated to PCP's operating with two-phase flow, showing the pressure

and temperature distributions along the pump stator under different sets of variables such as gas void fraction, rotational speed and delivered pressure. Bratu, 2005 performs experiments and describes the thermo-mechanical process and overheating generated when the gas phase is compressed within the pump cavities. The present work is part of an research program aimed at developing a better understanding of PCP's performance.

## 2. EXPERIMENTS

Figure 1 shows a schematic view of the test facility specially built for the experimental evaluation of the pump's performance, The working fluids were water and air. . The pump used in the tests had seven stages (cavities), and it was rated by the manufacturer to produce a maximum pressure difference between outlet and inlet sections of the order of 35 kgf/cm$^2$. The rotor diameter was 38 mm. The pump was operated by an induction motor connected to a frequency inverter, so as to allow for control of the rotational speed. A torque meter was installed on the shaft to measure the torque applied to the pump. The shaft rotational speed was obtained directly from the frequency inverter.

Water was fed to the pump by means of a two-tank system. A higher tank supplied water to the pump inlet by gravity. After passing through the pump, the water was discharged to the lower tank. A centrifugal pump was used to return the water to the upper tank. A return line connecting the upper to the lower tank was installed and used to keep the water level in the upper tank constant. Downstream of the pump, a valve was installed to restrict the flow out of the pump and produce the different levels of pressure difference across the pump needed for the tests. A pressure relief valve was also installed in the water circuit for safety reasons. A calibrated turbine meter was employed to measure the water flow rate admitted into the pump.

For the two-phase flow tests, compressed air from the laboratory was supplied to the pump. The air was injected through two opposing ports directly into the first cavity of the pump. To this end, holes were drilled through the stator casing and rubber body. The supplied air flow rate was measured by a calibrated rotameter. Inlet temperature and the pressure measured within the first cavity were used to determine the air density. By the water and air supply system employed, the two phase flow was formed within the first cavity of the pump.

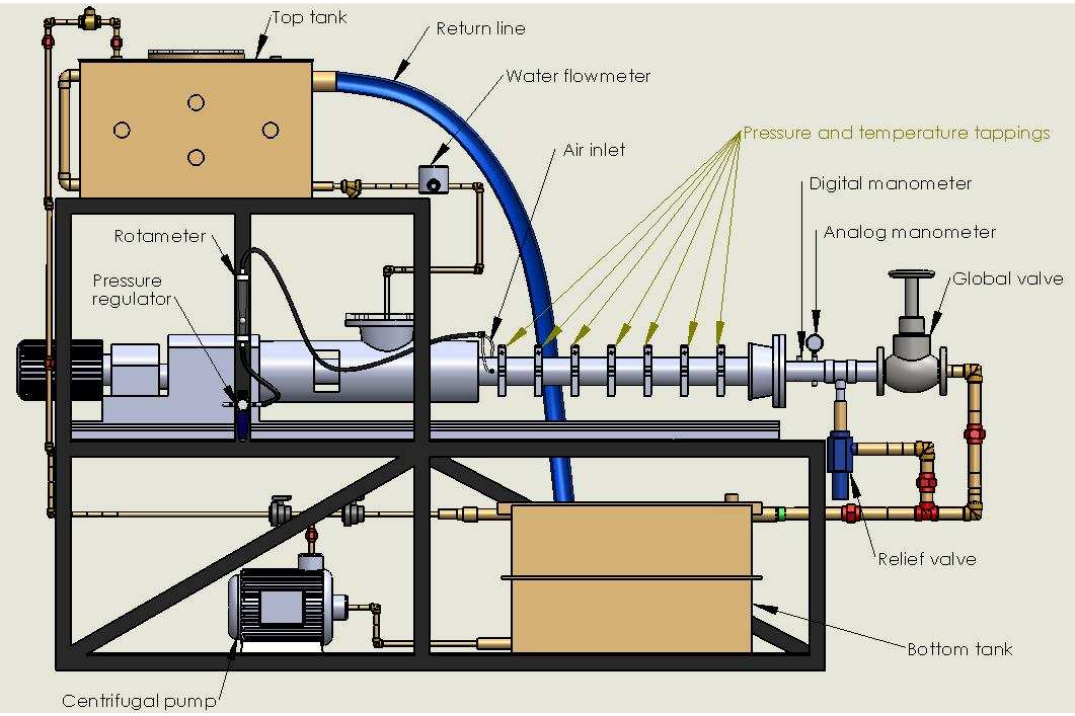


Figure 1. Schematic view of the test section employed in the experiments.

Since the main objective of the study was to produce detailed information on the pump performance, pressure and temperature sensors were installed within each cavity of the pump. Special mounts were designed and constructed to provide access of the temperature and pressure sensors to the cavity space, Figures 2, 3 and 4 were prepared to help describing the mounts constructed for the probes. After the stator steel casing and rubber body had been drilled at pre-determined axial locations, the two half of the mounts were installed around the steel casing. The vertical hole in the mount was aligned with the hole in the casing. Through this hole the small diameter steel pipe soldered to a flange shown in Fig. 3 was inserted penetrating the stator rubber, but not protruding to the interior of the cavity, so as not to touch the rotor surface. The tube had one end closed and received a fine gauge thermocouple through its other end. The diameter of the steel tube was smaller than the hole in the stator case and in the mount, so that fluid from the interior of

the cavity could communicate with the horizontal hole drilled in the upper part of the mount. A pressure transducer was installed at one end of this horizontal hole. The other end receives a sealing plug, and it was used for purging the system when necessary.

.

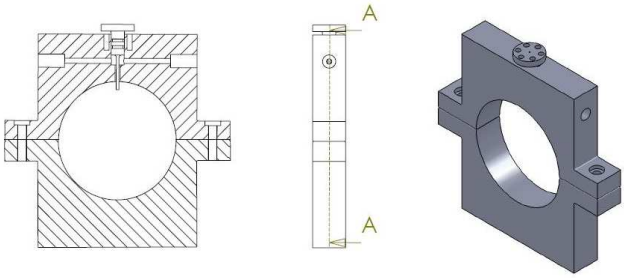


Figure 2. View of the mounts for the pressure and temperature sensors.

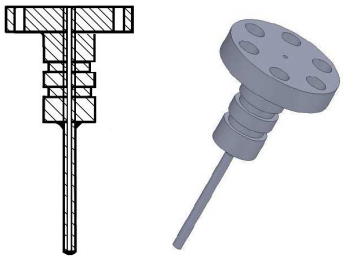

Figure 3. Flange and tube assembly for the thermocouple temperature sensor

One mount equipped with pressure and temperature sensors was installed at the location of each pump cavity. These locations are indicated in Fig. 3 that shows a cross section view of the pump stator. The axial locations were chosen so as to coincide with the positions where the thickness of the stator rubber were minimum. An additional pressure sensor was installed at the exit section of the pump.

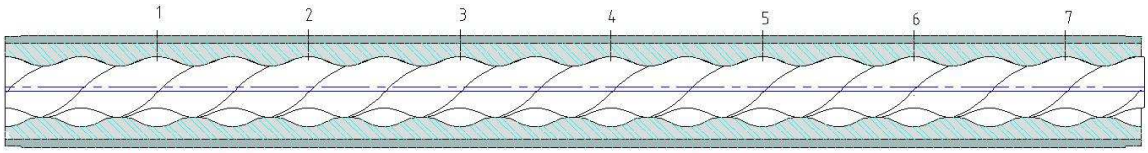


Figure 4. Stator cross section view showing the location of pressure and temperature sensors.

All the sensors descried previously were connected to a data acquisition system for data processing and recording. Figure 5 shows two photographs of the test section constructed.

In the case of the liquid experiments, the pump rotational speed was set and a particular value for the inlet-to-outlet pressure difference, ΔP, was set by manually adjusting the position of the downstream flow control valve. After a few minutes, a steady sate condition was achieved and the data for torque, volume flow rate, pressure and temperature axial distributions were recorded by the acquisition system. For the two-phase experiments the gas volume fraction at the first cavity was also set for each experiment. The following definition for GVF was adopted, where $Q_{air}$ and $Q_{water}$ stand, respectively for the volume flow rates of air and water,

$$\alpha = 100.\frac{Q_{air}}{Q_{air} + Q_{water}}$$

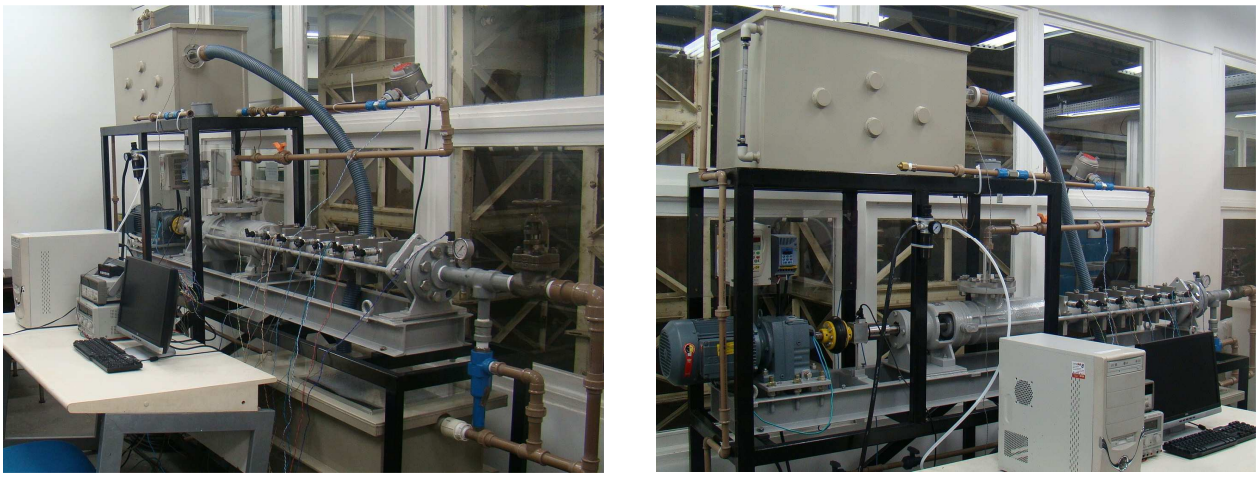

Figure 5. Photographs of the test section showing the PCP and measuring setup.

## 3. RESULTS

The experimental results obtained will be presented starting with the liquid flow experiments and followed by the two phase flow experiments

### 3.1. Liquid Flow Experiments

**Volumetric Flow Rate.** Figure 6 presents the results for liquid volumetric flow rate versus pressure for the pump tested, for rotations equal to 50, 98 and 168 RPM, The gauge pressure range tested was from 0 to 35kgf/cm$^2$, the maximum rated pressure for the pump employed.

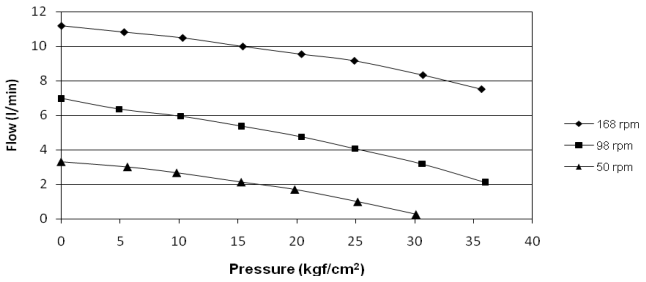


Figure 6. Volumetric flow rate vs. pressure differential along the pump, for three different shaft speeds.

An observation of the results shown in the figure indicate an expected trend for PCP's operating with liquids. For a fixed rotational speed the volume flow rate pumped decreases with the pressure difference. For flexible stator materials, higher downstream pressure levels induces a back flow from the downstream cavities toward the upstream cavities due to the loss of sealing between the stator and the rotor. For higher speeds this effect is relatively less pronounced due to the axial momentum delivered to the fluid. For the lower speed tested, one can observe that the PCP ceased to pump fluid.

**Pressure Axial Profile.** Figure 7 shows the measured pressure axial distribution along the pump using the sensors installed at each pump stage, or cavity. The figure shows curves of pressure distribution at a fixed rotation of 98 RPM and for different levels of downstream. Pressures are indicated in each of the seven stages of the pump and at the output (position 8 in the figure).

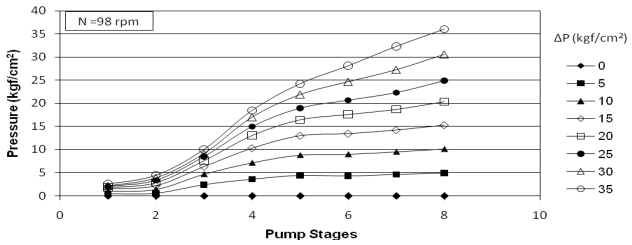


Figure 7. Pressure distribution for single phase flow at various differential pressures for shaft speed of 98 RPM.

An analysis of figure above indicates that, even for the lower operating pressure level of 5kgf/cm$^2$, there is communication between the cavities (stages) of the pump due to the pressure field generated in the stator-rotor gap by back flow. In fact, observing the curve corresponding to the output pressure of 5kgf/cm$^2$ it appears that the pressure is approximately constant over the last three pump stages and equal to the output pressure, 5kgf/cm$^2$.

This is an indication of a strong geometric communication between these cavities. For the cavities situated further upstream, one verifies a steep drop in pressure toward the pump inlet. Considering the liquid as an incompressible fluid, the increase in the pressure gradient observed in the cavities closest to pump inlet can be associated to smaller gaps between the rotor and stator. This behavior can be observed, even more pronounced, for the curves correspondents to higher discharge pressures levels.

An observation of the curves shows presented in the figure indicates that the seven pump stages of the pump tested are actually only necessary for operations where the outlet pressure exceeds 15 kgf/cm$^2$.

**Useful Power**. Figure 8 presents the results for the useful power supplied by the pump to the fluid for three values of the rotational speed. This quantity was obtained by multiplying the flow rate by the pressure difference across the pump.

The results show a significant increase in the useful power supplied to the liquid with the increasing rotational speed of the pump. For a fixed pressure difference these results are a consequence of the increase in volume flow rate commented before for the higher rotation speeds. For rotations speeds of 50 and 98 RPM a local maxima in the curves are observed. This behavior can be associated to the verified reduction of flow rate due to loss of sealing in the downstream cavities caused by the increased exit pressure at low rotational speeds. In the case of the higher rotational speed tested, 168 RPM, the presence of the maximum value is hinted by the results but not actually achieved, for the maximum exit pressure tested of 35kgf/cm$^2$.

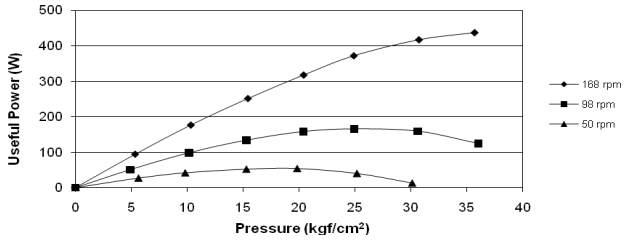


Figure 8. Useful power supplied to the fluid as a function of pressure differential and shaft rotational speed

**Delivered Power**. The power delivered to the pump was calculated by multiplying the torque measured at the shaft by the rotational speed. The results presented in Fig. 9 indicate a linear variation of the power delivered to pump with the exit pressure level, for the three different shaft speeds tested. As the power supplied to the fluid tends to drop with increasing exit pressure, as shown in Fig. 8, the linear increase of the power supplied to pump is an indication of the importance of the power consumed by friction between the rotor and stator and power lost to drive the back or slip flow.

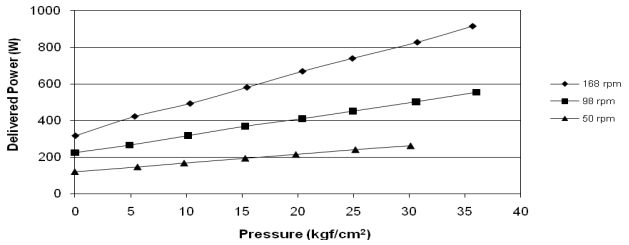


Figure 9. Delivered power to the pump as a function of pressure and shaft speed

**Pump Efficiency.** The ratio of the power delivered to fluid to that delivered to the pump provides the pump efficiency. Figure 10 presents the results for pump efficiency obtained for three rotations, as function of pump exit pressure.

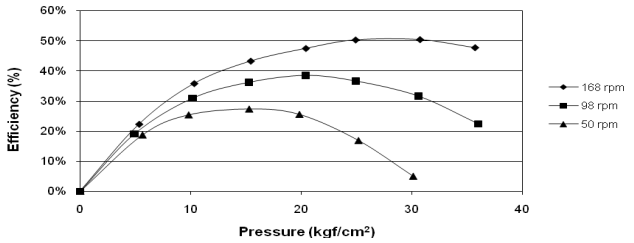


Figura 10. Pump efficiency as a function of pressure and shaft speed

A global observation of the results of Figure 10 indicates that pump efficiency increases with increasing shaft speed. This behavior can be rationalized by the fact that the power expended to overcome friction between rotor and stator is proportionally lower for larger rotations, as already commented.

As expected from the results previously presented, a maximum is displayed in the efficiency curve for each rotational speed. This result is a consequence of the decrease in the flow rate pumped with increased exit pressure.

**Pump Volumetric Efficiency.** Figure 11 shows the results obtained for the volumetric efficiency of the pump for three rotational speeds, as function to the exit pressure pump. Volumetric efficiency was determined as the ratio of the pumped flow rate actually measured by the theoretical value that the pump could produce at the same rotation. There

are two ways of determining the theoretical volume flow rate for a particular pump. It can be calculated from the drawings used to manufacture the pump, or else from measurements of the flow rate delivered at a condition of zero pressure difference across de pump. It is assumed that at this condition sealing is perfect between rotor and stator and, therefore, the pump delivers its maximum flow rate. In the present study these two values agreed to less than 1% for all rotational speeds tested.

The results of Fig. 11 show a monotonic decrease of volumetric efficiency with increasing exit pressure for all rotational speeds tested. For the same exit pressure, the volumetric efficiency is observed to be higher for higher speeds. This fact can be attributed to the increased axial momentum imparted to the fluid by the rotor at higher speeds, which is able to better overcome the adverse pressure gradient that prevails at the downstream cavities.

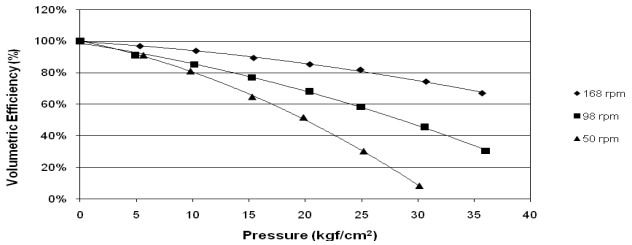


Figure 11. Pump volumetric efficiency as a function of exit pressure and shaft speed

**Slip Flow**. Slip flow is the reverse flow imposed by the adverse pressure gradient on the pump axial flow. Slip flow was calculated by subtracting the measured flow rate from the maximum theoretical flow rate at a particular speed and exit pressure level. The results for slip flow obtained are shown in Fig. 12 for the three tested rotations as function of the exit pressure. These results complement the comments made regarding Fig. 11. Indeed, smaller values of slip flow are observed for higher rotational speeds.

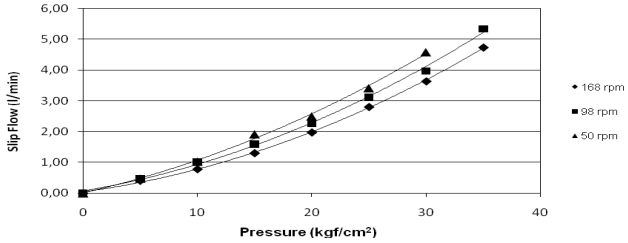


Figure 12. Slip flow as a function of pressure and shaft speed

**Temperature Profiles.** Figure 13 presents the temperature profiles obtained by measuring the temperature in each pump cavity. The results are presented for a speed of 130 RPM as a function of the exit pressure level.

The results indicate that the fluid temperature increases along the pump are small for all exit pressure values tested. The maximum increase observed was for the case of exit pressure of 30kgf/cm$^2$ which was less than 1ºC. There is, however, a tendency to increase the temperature level for higher exit pressure values. This result, however, is of limited interest since is related to the close loop operation mode employed in the test. Since the water reservoirs employed were limited, an increase in the temperature level of the water should be expected for a long term operation..

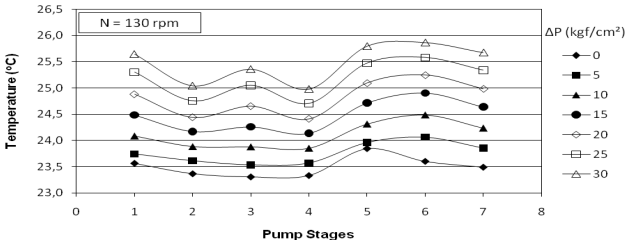


Figure 13. Temperature axial profile along the pump as a function of exit pressure for 130 RPM

### 3.2. Two Phase Flow Results

**Pressure Axial Profile**. Fig. 14 presents the measured pressure distribution along the pump for a rotation of 130 RPM, for gas void fraction (GVF) at the inlet of 50% and for different levels of exit. Pressures values are indicated at each of the seven stages of the pump and at output section (position 8 in the figure).

An analysis of the results presented shows that the communication between the pump cavities (stages) increases as the exit pressure increases. It is interesting to compare the results of Fig. 14 with those of Fig. 7 where the pressure profiles for the single phase case were presented. Such a comparison indicates that, for the same exit pressure level, the for the two phase case the cavities are sealed at positions farther downstream than for those for the single phase case. This result can be attributed to the compressibility of the two phase flow that accommodates the back flow produced by the adverse pressure gradient at the downstream cavities, without propagating its effect to far upstream.

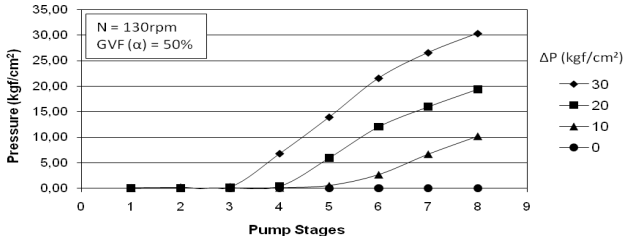


Figure 14. Pressure distribution along the pump for 130 rpm and 50% GVF

The pressure profiles can be seen in an alternative plot, as presented in Fig. 15. In this figure, the pressure profiles are shown for different values of GVF at the pump inlet, for a fixed exit pressure and rotational speed. The effect of decreasing pressure communication among the cavities with increasing GVF is clearly seen in the results. It can be noted that even for this higher value of the exit pressure there is perfect sealing of the first pump cavity, for the higher GVF values.

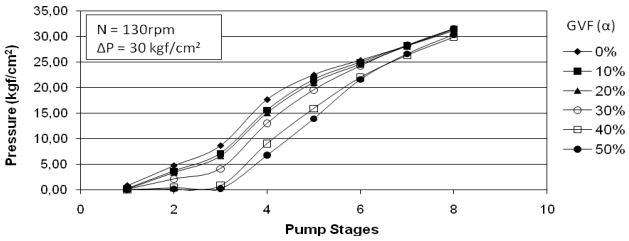


Figure 15. Pressure distribution along the pump for 130 rpm and 30kgf/cm² ΔP

**Useful Power**. Figure 16 shows the results for the useful power supplied to the fluid by the pump at rotation of 130 RPM, and for different GVF values of 0, 10, 20, 30, 40 and 50%. The presence of air in the mixture pumped causes a decrease in the power supplied to the fluid due to decreased volume flow and density of the mixture as the GVF is increased.

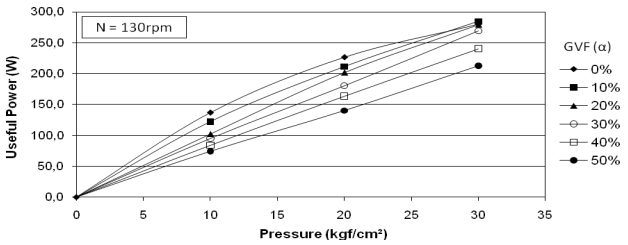


Figure 16. Useful power supplied to the fluid by the pump at 130 RPM and for different GVF values

**Delivered Power**. The shaft power delivered to the pump is shown in Figure 17 for 130 RPM and the different values o GFV indicated. It can be observed from the results of the figure that the fraction of air in the mixture does not exert a significant influence on the power supplied to the pump. This result can be an indication that the torque required to drive the rotor within the stator is a relevant part of the total torque provided.

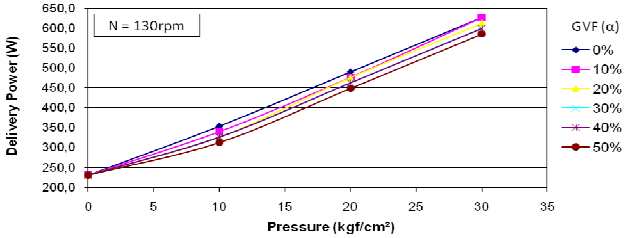


Figure 17. Delivered power supplied to the pump at rotation of 130 RPM and for different GVF values

**Pump Efficiency**. Figure 18 shows the results for the pump efficiency at 130 RPM and for the different GVF values indicated. The results allow a comparison of pump efficiency operating with single phase flow (water, $\alpha = 0$) and those with increasing air fraction. A sharp decrease in pump efficiency with the gas void fraction increase can be observed. It is noted that the difference between the efficiency of single-phase flow and multiphase flow tends to decrease as the exit pressure increases. This fact can be associated with increased density of the gas phase with the pressure at this location in the pump.

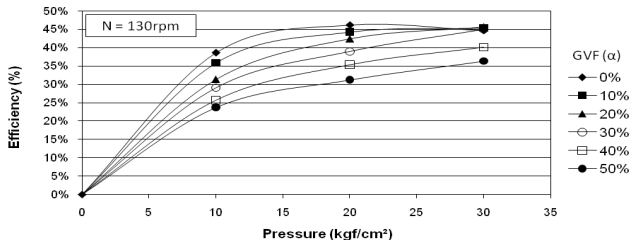


Figure 18. Pump efficiency at 130 RPM and for different GVF values

**Volumetric Efficiency.** Figure 19 shows the results for the pump volumetric efficiency at 130 RPM and for different GVF values indicated. The volumetric efficiency of the PCP is a strong function of the mixture compressibility. In fact, the greatest differences in volumetric efficiency between single-phase and multiphase flow operations are found in experiments where the gas void fractions are higher and the operating pressures are lower. Under these conditions the mixture is higly compressible, which causes a decreases in volumetric efficiency. For higher levels of exit pressure, the difference in volumetric efficiency is lower due to the higher density of the gas phase.

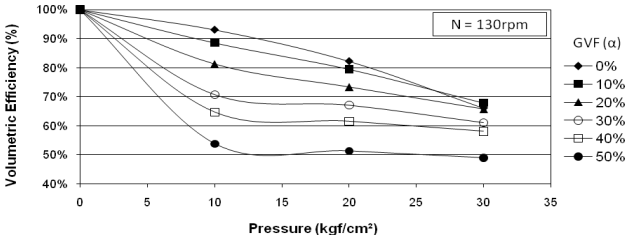


Figure 19. Pump volumetric efficiency at 130 RPM and for different GVF values

**Slip Flow.** Figure 20 shows the results for the slip flow through the PCP at 130 RPM and for the different GVF values indicated. The results in figure should be interpreted with caution for multiphase flow case, since the gas compressibility accommodates part of the return flow of the liquid phase, which does not necessarily mean a liquid flow across the pump against the main stream, as it is the case of the single-phase operation with liquid. The results of Fig. 20a are presented in a bar graph format in Fig. 20b, where we can verify the lower sensibility of slip flow to the exit pressure, as the void fraction increases.

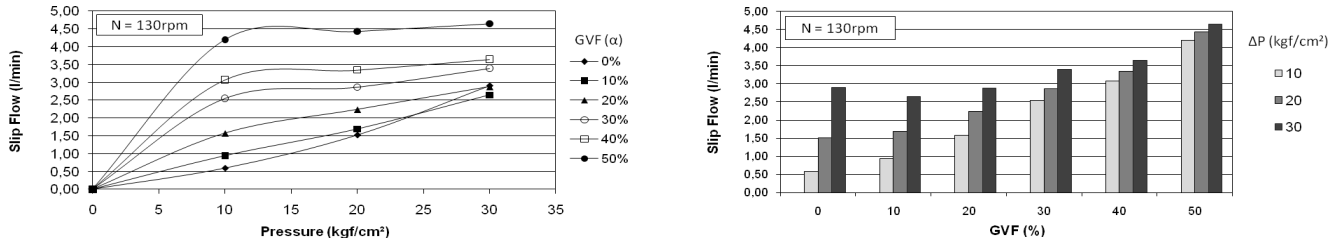


(a) (b)

Figure 20. (a) Slip flow through the PCP at 130 RPM and for different GVF values. (b) Slip flow through the PCP for different pressure levels as function of GVF

**Torque Supplied**. Figure 21 shows the results for the torque supplied to the PCP at 130 RPM and for the different GVF values indicated. It is observed from the figure that the torque supplied to the pump is mainly determined by the operating pressure and it is a weak function of the GVF.

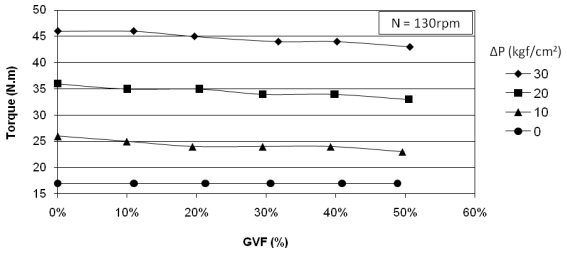


Figure 21. Torque supplied to the pump at 130 RPM and for different GVF values

**Gas Void Fraction**. Figure 22 shows the gas void fraction behavior along the pump stages at 130 RPM under zero operating pressure difference (ΔP = 0). It canbe seen that, due to the perfect seal between rotor and stator, the pressure and the gas void fraction are kept constant in the multiphase flow through the pump.

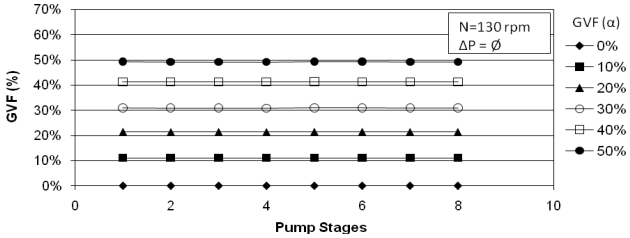


Figure 22. Gas void fraction behavior along the pump stages at 130 RPM under zero operating pressure difference.

As the pressure at the pump output is progressively increased, the GVF of cavities submitted to higher pressure levels decreases sharply due to the effect of the gas compressibility. The GVF variation along the pump stages can be seen in Fig. 23, for a 50% GVF measured in the first cavity.

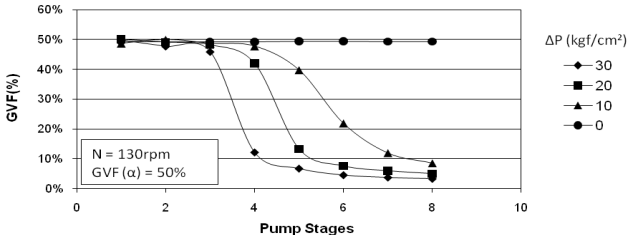


Figure 23. GVF behavior along the pump for different exit pressure levels at 130 RPM., and for 50% GFV at the inlet.

**Temperature Profile.** Figure 24 illustrates the measured temperature profiles along the pump at 130 RPM under 20kgf/cm$^2$ of exit pressure, and for the different GVF values indicated. The results indicate that the mixture temperature decreases in the first cavity. . This cooling effect is probably associated to the gas expansion and water absorption by air, which requires absortion of latent heat for the phase change to take place. The mixture temperature is seen to

increase as it flows along the cavities as higher pressure levels prevail. This heating can be associated to the work of compressionof the air, but also to the heat generated by the friction between the rotor and stator that eventually is transferred to the fluid. It should be noted that, although temperature variations along the pump were measured, the overal temperature variation from inlet to outlet is not significant.

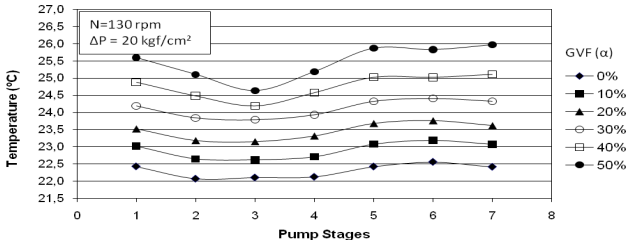


Figure 24. Temperature behavior along the pump at 130 RPM under operating pressure of 20kgf/cm$^2$

## 4. CONCLUSIONS

The work conducted an experimental study of a Progressive Cavity Pump operating with water and with a two phase flow of air and water. An experimental test section was designed and constructed to allow the measurement of relevant information on the pump performance. The experiments measures the pump rotational speed, torque, volume flow of each phase, as well as temperature and pressure. For singlephase flow, even for the lower operating pressure, there is communication between the pump cavities due to the pressure field generated in the stator-rotor gap by returning flow. Considering that the power supplied to the fluid drops from a given output pressure, the linear increasing of the power supplied to pump is an indication of importance of the power consumed by friction between the rotor and stator. The power expended to overcome the friction between the rotor and stator is proportionally lower for larger rotations, compared to useful power delivered to the fluid. The increased axial momentum delivered to the fluid in operations with higher speeds allows the fluid to win the adverse pressure gradient imposed to the flow by the high pressure at the exit. As the pressure at the pump output is progressively increased, the GVF of cavities submitted to higher pressure levels decreases sharply due to the effect of gas compressibility. The communication between the pump cavities (stages) decreases as well. The presence of air into the mixture pumped causes a decrease in power supplied to the fluid. The gas compressibility accommodates part of the return flow of the liquid phase, which does not necessarily mean a liquid flow across the pump against the main stream flow, as in the case of the single-phase operation with liquid.The mixture temperature decreases in the first cavities due to gas expansion and water absorption by air, and than consequent phase change of latent heat absorption. The mixture temperature is increased as it goes through the cavities with higher pressure levels. The heating is related to the work of the air compressing in the mixture.

## 5. REFERENCES

Gamboa J., Olivet A. and Espin, S., 2003. “New Approach for Modeling Progressive Cavity Pumps Performance”, SPE SPE 84137, Annual Technical Conference and Exhibition , Denver, , U.S.A.

Martin A.M., Kenyery F. and Tremante A., 1999. “Experimental Study of Two Phase Pumping in Progressive Cavity Pumps”, SPE Latin American and Caribbean Petroleum Engineering Conference, SPE 53697, Caracas, Venezuela.

Bratu C., , 2005. “Progressing Cavity Pump (PCP) Behavior in Multiphase Conditions”, SPE 95272, SPE Annual Technical Conference and Exhibition, Dallas, , U.S.A.